Cellulose (2024) 31:10879–10894
https://doi.org/10.1007/s10570-024-06181-4

ORIGINAL RESEARCH

Improving tribological efficiency of isopropyl palmitate oil with cellulose nanocrystals: a sustainable approach for high-performance lubricants

María J. G. Guimarey · Marco A. Marcos · Javier P. Vallejo · José L. Viesca · María J. P. Comuñas · Luis Lugo · Antolin Hernández Battez

Received: 27 April 2024 / Accepted: 18 September 2024 / Published online: 2 November 2024

Abstract This article explores the potential of cellulose nanocrystals (CNCs) as a lubricant additive for isopropyl palmitate (IPP) oil to enhance its tribological performance. CNCs, derived from renewable sources, offer a sustainable and environmentally friendly alternative to traditional lubricant additives. A two-step method was used to prepare the nanolubricants, with visual control and dynamic light scattering measurements to assess their temporal stability. The viscous behavior of the nanolubricants, in terms of viscosity and viscosity index, was evaluated at different temperatures. The study assesses the effectiveness of CNC/IPP oil blends as lubricants through tribological tests, including evaluations under pure sliding and rolling–sliding conditions. Studies on worn surfaces were conducted using surface roughness analysis, Raman mapping, and XPS, and the thermal stability was examined to determine their suitability for different operating conditions. CNCs significantly reduce friction by up to 44% and improve wear resistance compared to the neat IPP base oil, presumably due to a self-repairing effect. Furthermore, an improvement of the thermal conductivity of pure IPP base oil has been revealed with increasing CNC concentration. This study enhances the understanding of cellulose nanocrystals as lubricant additives and their potential to transform traditional lubricating oils into high-performance and sustainable solutions.

Supplementary Information The online version contains supplementary material available at https://doi.org/10.1007/s10570-024-06181-4.

M. J. G. Guimarey (✉) · M. J. P. Comuñas
Laboratory of Thermophysical and Tribological Properties, Nafomat Group, Department of Applied Physics, Faculty of Physics, University of Santiago de Compostela, 15782 Santiago de Compostela, Spain
e-mail: mariajesus.guimarey@usc.es; mgarciaguimarey@bournemouth.ac.uk

M. J. G. Guimarey · J. L. Viesca · A. H. Battez
Department of Design and Engineering, Faculty of Science & Technology, Bournemouth University, Poole, Dorset BH12 5BB, UK

M. A. Marcos
IDMEC, Instituto Superior Técnico, University of Lisbon, 1049-001 Lisbon, Portugal

M. A. Marcos · L. Lugo
Department of Applied Physics, University of Vigo, 36310 Vigo, Spain

J. P. Vallejo
Centro Universitario de la Defensa en la Escuela Naval Militar, Grupo InTeam, Plaza de Spain, S/N, 36920 Marín, Spain

J. L. Viesca (✉) · A. H. Battez
Department of Construction and Manufacturing Engineering, University of Oviedo, Asturias, Spain
e-mail: viescajose@uniovi.es

Keywords Cellulose nanocrystal · Isopropyl palmitate oil · Friction · Wear

Introduction

The lubricant industry is under pressure to reduce its environmental impact due to concerns such as resource depletion, pollution, and the need for biodegradable alternatives (Li et al. 2019). Conventional lubricants, which are often derived from non-renewable petrochemical sources, contribute to environmental degradation during their production, use, and disposal (Madanhire and Mbohwa 2016). In response to this, numerous legislative initiatives are being implemented worldwide. Thus, the European Union approved Commission Decision (EU) 2018/1702 establishing the EU Ecolabel criteria for lubricants. This EU Ecolabel guarantees that the lubricants have a limited impact on the aquatic environment, contain a restricted number of hazardous substances and perform as well as or better than a conventional lubricant available on the market.

In this context, there is an increasing interest in plant-based lubricants. These lubricants possess biodegradable properties, which reduce the persistence of lubricant residues in the environment, and show excellent tribological properties (Madanhire and Mbohwa 2016; Woma et al. 2019). However, their limited thermo-oxidative stability still requires improvement (Fox and Stachowiak 2007; Yosief et al. 2023). In this regard, the saturated fatty acid ester, isopropyl palmitate (IPP), is a notable candidate to be used as base oil in the formulation of plant-based lubricants due to its biodegradability, low toxicity, and sustainable supply potential. As a saturated ester, IPP is less prone to oxidation compared to unsaturated oils or esters and its thermo-oxidative stability is greater than plant-based oils (Kodali 2002).

Additives derived from cellulose include cellulose nanocrystals (CNCs) and cellulose nanofibrils (CNFs). These additives possess high surface area, hydrophilic properties, and the ability to form robust films on metal surfaces (Aryasena et al., 2022; Awang et al. 2019a, b). As a result, they represent a promising option for improving the tribological performance of plant-based lubricating base oils while maintaining their original environmental properties. Furthermore, since cellulose is the most abundant polymer in nature, these derived additives would be readily available at an industrial scale.

Cellulose derivatives have been studied as additives in water-based fluids for application in cutting or lubricating fluids (Da Rocha et al. 2022; Liu et al. 2022). Similarly, cellulose esters (Zhang et al. 2018) and cellulose nanoadditives have been used as lubricating oil additives. Li et al (2019) have studied the incorporation of cellulose nanocrystals (CNCs) and surface modified cellulose nanocrystals (mCNCs) into polyalphaolefin (PAO) base oil as lubricant additive. The PAO/mCNC nanolubricants obtained showed by visual control a dispersive stability of up to 5 h. These researchers concluded that incorporating mCNC additives not only enhances lubricants viscosity, thereby improving the formation of a lubricant film in boundary lubrication but also significantly reduces both friction and wear by mending surface roughness. Fernández-Silva et al. (2021) investigated the rheological and tribological behavior of fibrillated or cellulose nanocrystals in vegetable oil, specifically castor oil, high oleic sunflower oil or their mixtures. The stability of the designed nanolubricants was not reported. The authors found that the tribological behavior of ecolubricants depends more on the base oil than on the concentration of nanocellulose. Awang et al. (2019a, b) explored the tribological performance of CNCs as green additives in an engine oil (SAE40). Stability validation was reported by sedimentation observation after 3 weeks of preparation for all the concentrations. This study reveals that the mixing of CNC nanoparticles in engine oil significantly reduces the friction and wear rate and hence improves the lubricating properties of engine oil. Table 1 provides a summary of the articles that have focused on the use of nanocelluloses (CNCs, CNFs, etc.) as additives in lubricating oils. Furthermore, Pownraj and Valan Arasu (2021) have recently published a review article on the thermophysical, tribological, and stability characterization of nanoparticles in lubricants. The authors report that only 10% of nano-lubrication publications employ biological oils, with just 12% reporting both tribological and thermophysical properties of these systems. Thus, this research aims to investigate both tribological and thermophysical characteristics of a biological oil enhanced with novel green nanoadditives, CNCs, that have yet to be extensively explored. Kumar and Garg recently published a dispersion stability analysis and tribological evaluation

Table 1 Summary of cellulose nanomaterials as lubricant additives

Nanoadditive	Base lubricant	Size / nm	Optimum concentration	Temporal stability	Stability technique	Wear reduction / %	Lubrication mechanisms	Reference
CNC mCNC	PAO	–	2 wt%	5 h	Sedimentation observation	41	Mending effect	Liet al (2019)
CNC CNF	Castor oil High oleic sunflower	10–20	3.3 wt%	–	–	36.7 40	–	Fernández-Silva et al. (2021)
CNC	SAE40	75	0.1 wt%	3 weeks	Sedimentation observation	69	Mending and polishing effects	Awang et al. 2019a, b; Awang et al. 2019a, b

of a novel vegetable oil-based ionanolubricants (Kumar and Garg 2023a, 2023b, 2024a, 2024b).

This takes a novel look at the use of cellulose nanocrystals (CNCs) as additives in an isopropyl palmitate (IPP) base oil to formulate lubricants compliant with EU Ecolabel standards for low environmental impact. The findings suggest a promising avenue for transforming lubrication technologies towards greener and more sustainable practices.

Experimental details

Materials

Cellulose nanocrystal (CNC) nanoparticles were used as additives at mass concentrations of (0.25, 0.5, 0.75 and 1.0 wt%) to formulate nanolubricants based on isopropyl palmitate (IPP). The CNC, also known as Nanocrystalline Cellulose (CAS number 9004-34-6), is a crystalline form of cellulose composed of nano-sized cellulose fibrils extracted mainly from woody biomass. The CNCs were purchased from Nanografi Nano Technology (Ankara, Turkey). The isopropyl palmitate, $(CH_3(CH_2)_{14}CO_2CH(CH_3)_2$, (CAS number 142-91-6) was provided by Thermo Fisher Scientific (Waltham, MA, USA). IPP, a saturated fatty acid oil, has a viscosity index (VI) of 176 and kinematic viscosity of 5.23 and 1.90 $mm^2\ s^{-1}$ at 313.15 K and 373.15 K, respectively. These properties were measured using a Stabinger Viscometer SVM 3000 (Anton Paar, Graz, Austria). Table 2 summarizes the main properties of the acquired CNC and IPP samples.

Nanolubricant stabilitys

Before each test, the dispersions of CNCs in IPP underwent a two-hour ultrasonic bath and were

Table 2 Physical properties of CNC nanoadditive and IPP base oil, according to the manufacturers

Cellulose nanocrystal (CNC)	Provider	Nature	Density/ kg m^{-3}	Bulk density/ kg m^{-3}	Average particle size / nm	Decomposition temperature (TGA) / K	Crystallinity (XRD)
	Nanografi Nano Technology	Extracted from the woody biomass	1490	500–800	Wide: 10–20 Length: 300–900	622.15	92%
Isopropyl palmitate (IPP)	Provider	Nature	Density (293.15 K)/ kg m^{-3}	Melting point / K	Boiling point / K	Flash point / K	Purity
	Thermo Fisher Scientific	Vegetable	852	284.15–286.15	433.15	456.15	85%

then intermittently dispersed using 15–second pulses from a high-frequency ultrasonic disperser to prevent overheating. This process resulted in stable dispersion producing the CNC-based nanolubricant. The hydrodynamic size of cellulose nanocrystals dispersed in isopropyl palmitate was measured using a Zetasizer Nano ZS (Malvern Instruments, UK) and analyzed through dynamic light scattering (DLS) technique. The measurements determined the equivalent spherical diameter of the nanoparticles. To ensure optimal testing conditions, a diluted sample of 0.10 wt% of cellulose nanocrystals was used. The hydrodynamic diameter of the selected sample was measured over a period of 15 days to study the temporal stability of CNC/IPP. Two cuvettes were used, with approximately 1 milliliter of sample. One cuvette was kept static during the 15–day measurement period, while the other was shaken with a vortex for 30 s before each measurement. The measurements were taken at a scattering angle of 173° and at 298 K.

Viscosity and viscosity index measurements

The SVM 3000 Anton Paar rotational Stabinger viscometer was employed for the kinematic viscosity measurements following the ASTM D7042-04 standard. Kinematic viscosity was measured over a temperature range from 293.15 to 373.15 K, with measurements taken at intervals of 20 K. This equipment was also used to determine the viscosity index (VI), which indicates the change in fluid viscosity with temperature, following the ASTM D2270-04 standard. This standard provides a methodology for calculating the VI based on kinematic viscosity measurements at 313.15 K and 373.15 K.

Sliding friction tests

Sliding tests were conducted using an UMT–3 tribometer (formerly from CETR Corporation) in a reciprocating ball-on-disk configuration The balls used had a diameter of 6 mm, a hardness of 58–66 HRC, and a surface roughness of 0.05 µm (Ra). The disks had a diameter of 10 mm, a hardness of 225 HV30, and a surface roughness of 0.018 µm (Ra) and were made of AISI 52100 steel. The tests were conducted at 393.15 K and at 10, 20, and 30 N–load, corresponding to maximum contact pressures of 1.43, 1.80, and 2.06 GPa, respectively. The frequency used was 15 Hz, with a stroke length of 4 mm, and a duration of 60 min. Approximately 1 mL of lubricant was used for each sliding test. Each test was repeated at least three times. Before and after each test, the ball and disk specimens were cleaned in an ultrasonic bath with heptane for 5 min, rinsed with ethanol, and dried with hot air.

Worn surface analysis

The wear volume and surface roughness of the disk were measured using a confocal microscope (Leica DCM 3D), and the wear rate was determined. To characterize the wear surface, the worn surfaces of the steel disks were evaluated using confocal Raman microscopy (WITec alpha300R+) and for elemental and chemical state information by X-ray photoelectron spectroscopy (XPS). Photoelectron spectra were acquired using a Thermofisher NEXSA spectrometer equipped with a hemispherical electron analyzer and a micro-focused monochromatic Al Kα x-ray source (1486.6 eV).

Rolling-sliding tests

The tribological behavior of nanolubricants across various lubrication regimes was investigated using a Mini Traction Machine tribometer (MTM2) from PCS Instruments, configured in a ball–on–disk setup. Stribeck curves for the nanolubricants were recorded with a slide-to-roll ratio (SRR) set at 50%, a 50 N load (equivalent to a maximum contact pressure of 1.15 GPa), and a mean entrainment speed ranging from 2500 to 10 mm s^{-1}. Speed variations were tested at decrements of 100 mm s^{-1} from 2500 to 100 mm s^{-1} and in decrements of 10 mm s^{-1} from 100 mm s^{-1} to 10 mm s^{-1}. The experiments were conducted at temperatures of 313.15, 333.15, 353.15, 373.15, and 393.15 K. A volume of 10 mL of lubricant was used for each test. To evaluate the repeatability of the specified test profile on this apparatus, three trials were conducted utilizing a reference oil. The resulting friction coefficients exhibited a discrepancy of less than 10%, substantiating the repeatability of the MTM2 tests with the used test profile.

The rolling-sliding tests utilized perforated balls (Ø = 19.05 mm, 800–920 HV and Ra ≤ 0.02 µm) and standard disks (Ø = 46 mm, 720–780 HV and Ra ≤ 0.02 µm), both made from AISI 52100 steel.

Prior to and following the tribological tests, the specimens were cleaned with heptane in an ultrasonic bath for 5 min and then dried with hot air.

Thermal conductivity

Thermal conductivity was measured using a Thermtest THW-L2 (Thermtest Inc., Hanwell, NB, Canada) from 293.15 to 333.15 K, employing the transient hot wire technique as per ASTM D7896-19 (''ASTM International. ASTM D7896-14 Standard Test Method for Thermal Conductivity, Thermal Diffusivity and Volumetric Heat Capacity of Engine Coolants and Related Fluids by Transient Hot Wire Liquid Thermal Conductivity Method'' 2014). The manufacturer's stated that accuracy for thermal conductivity determinations with this device is 5% (Cabaleiro et al. 2020). The probe wire is 60 mm long and has a diameter of approximately 0.1 mm and is fully immersed in approximately 20 mL of the sample during testing. The temperature was controlled using an IC20XR dry bath (EchoTherm). To avoid natural convection phenomena, we selected a low thermal power and a short input time of 75 mW and 1 s, respectively, when conducting the measurements.

Results and discussion

Morphological and structural characterization

The morphology of the CNC nanoadditives was analyzed using transmission electron microscopy (TEM) with a JEM–1010 microscope from JEOL (Tokyo, Japan) operating at 100 kV. Figure 1 shows representative images of the CNC nanoparticles. The fibril shape is clearly observable, and the obtained dimensions are in good agreement with those of the manufacturer (length: 300–900 nm, width: 10–20 nm).

The structure of the CNC nanoadditive and IPP lubricant were characterized by Raman spectroscopy in the range of 0–3500 cm^{-1} through a WITec Alpha300R confocal Raman microscope with a 532–nm excitation laser diode (Ulm, Germany). Figure 2 shows the Raman spectrum of the CNC nanoadditive and of the IPP base oil. The first is characterized by the presence of vibrations signals about 1099 cm^{-1}, which are attributed to CH and CH_2 stretching and asymmetric stretching vibration of the C–O–C glycosidic linkage. The characteristic peaks at 1480 cm^{-1} and at 1384 cm^{-1} are associated with H–C–H and H–O–C bending, respectively (Satha et al. 2020). The Raman spectrum of the IPP base oil indicates the characteristic absorption bands: CH_2 deformation in lipid and CH_3 twisting at 1298 cm^{-1}, CH_2CH_3 deformation at 1444 cm^{-1}, stretching of ester (C=O) in lipid at 1737 cm^{-1}, cm^{-1} symmetric stretch of CH_2 (in lipid) at 2853, symmetric stretch of CH_3 at 2890 cm^{-1}, and asymmetric stretch of CH_2 at 2927 cm^{-1} (Roohpour et al. 2009).

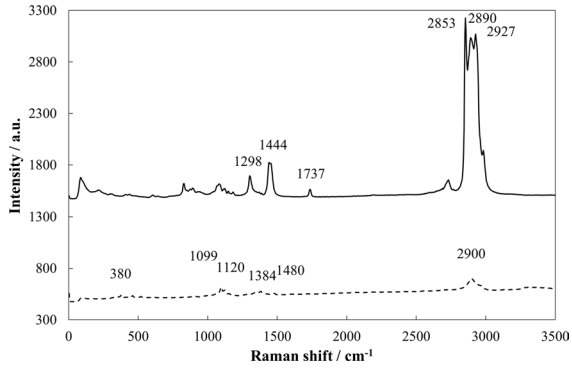

Fig. 2 Raman spectrum of the CNC nanoparticles (dashed line) and IPP base oil (continuous line)

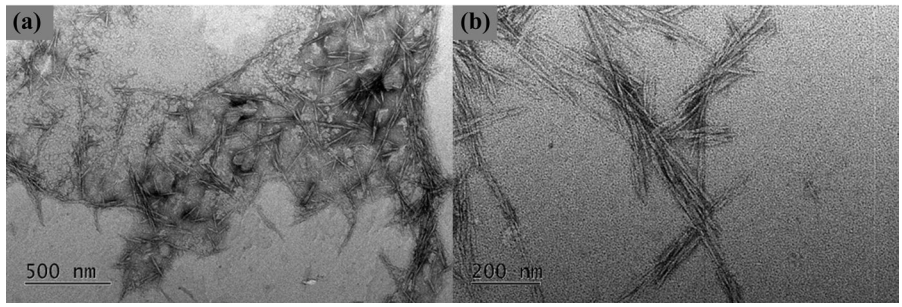

Fig. 1 TEM images of the CNC nanoparticles at 500 nm (**a**) and 200 nm (**b**) scale

Nanolubricant stabilities

Figure 3a shows the size evolution of cellulose nanocrystals (CNCs) dispersed in IPP, under static and shaken conditions. The morphology of CNCs includes dimensions several times larger in one of their axes, which may result in measured diameter values closer to the length value of the nanoparticles. Several authors (Marcos et al. 2018; Marcos et al. 2020; Marcos et al. 2023) reported different dimensions determined under microscopy and DLS. It is important to note that microscopy examines dry samples, while DLS characterizes hydrodynamic diameters (Vallejo et al. 2019). The figure illustrates a decrease in size over time for the static sample, indicating some signs of precipitation of the largest nanoparticles in the days after sample preparation. In contrast, the sample subjected to shaking conditions maintained a stable size of approximately 1340 nm, which suggests that the presumed precipitation did not lead to the formation of undesired aggregates of nanoparticles, facilitating the attainment of the initial conditions.

Figure 3b displays the nanoparticle size distributions obtained for the sample immediately after preparation, as well as its distribution after 15 days both under static conditions and for agitated conditions. The precipitation of the nanocrystals is a result of a slight deposition with gravity. However, the initial dispersion conditions can be easily restored through simple mechanical shaking, even after standing motionless for several days. In previous works in which CNCs were used as lubricant additives in oils, stabilities were only evaluated by observing sedimentation, obtaining stabilities of less than one day (5 h) for surface-modified CNCs (Li et al 2019) and at most 3 weeks for CNCs in engine oil (Awang et al. 2019a, b). Our experimental study reveals similar nanolubricant stabilities but including a deeper assessment which conclude a dispersion recovery with a slight agitation. The images of static and shaken samples after freshly dispersed samples (0 h) and finished DLS tests (15 days) are shown in Figure S1. As can be seen, the static sample after 15 days shows a clear transparency that may be due to possible precipitation of the CNCs. However, the shaken sample at 15 days shows a slight turbidity like that observed in the freshly prepared samples (0 h).

Viscous behavior

Figure 4a shows the kinematic viscosity for the IPP base oil (0 wt%) and for all CNC/IPP nanolubricant concentrations at different temperatures. As can be observed, at low CNC concentrations, the kinematic viscosity remains unchanged or slightly decreases compared to that of IPP base oil. However, at high concentrations and low temperatures, the kinematic viscosity increases with respect to that of IPP. For example, the viscosity at 293.15 K is 8.54 $mm^2\ s^{-1}$ and 8.72 $mm^2\ s^{-1}$ for the IPP base oil and for the nanolubricant with 1 wt% CNCs, respectively. This trend reverses with increasing temperature. For example, at 373.15 K the kinematic viscosity is 1.89 $mm^2\ s^{-1}$ for IPP base oil and 1.84 $mm^2\ s^{-1}$ for the nanolubricant with higher CNC concentration. Kinematic viscosity values for the IPP base oil and all nanolubricants are gathered in Table S1.

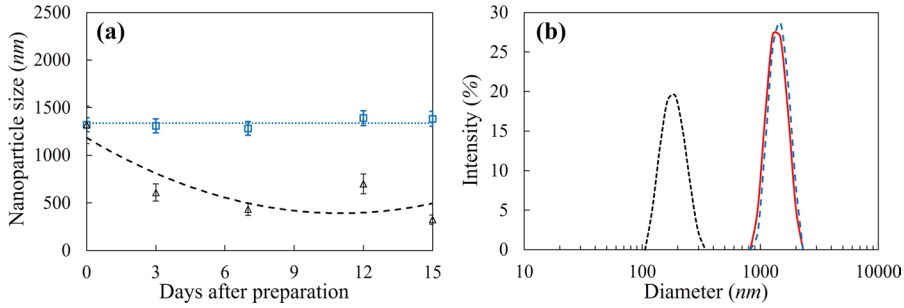

Fig. 3 (**a**) Temporal evolution of the hydrodynamic diameter for the 0.10 wt% CNC/IPP nanolubricant under shaken (blue square) and static (triangle) conditions. Error bars indicate the uncertainty regarding experimental data for shaken and static samples, respectively; (**b**) Hydrodynamic size distribution by intensity of CNCs just after preparation (red line), and after 15 days for shaken (dashed blue line) and static (dashed line) conditions

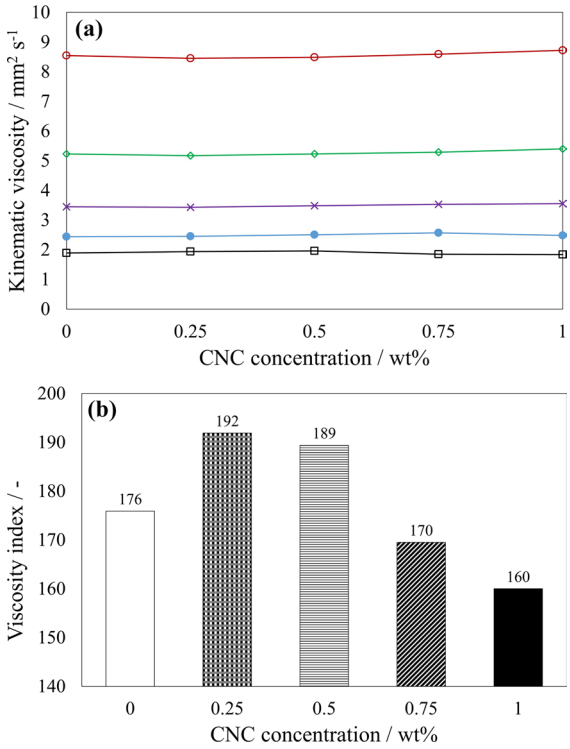

Fig. 4 (**a**) Kinematic viscosity measurements for the IPP base oil and CNC concentrations at different temperatures: 293.15 K (red ring), 313.15 K (green diamond), 333.15 K (violet coloured X), 353.15 K (blue filled circle) and 373.15 K (square); (**b**) Viscosity index values

Figure 4b shows the viscosity index (VI) for the IPP base oil and the different CNC/IPP nanolubricant concentrations. At low concentrations of CNCs, the VI increases compared to that of IPP base oil, reaching a 9% increase for the lowest CNC concentration (0.25 wt%). However, at high concentrations, there is a decrease in VI relative to the base oil, with a 9% reduction observed for the highest concentration (1.0 wt%). This could be attributed to potential transitory CNC agglomeration at higher concentrations, which can lead to a non-uniform distribution within the oil. This potential transitory agglomeration can disrupt the lubricant's flow properties and increase sensitivity to temperature changes, thus reducing the VI. This highlights the importance of optimizing CNC concentrations to achieve desired lubricant performance.

Table 3 Average coefficient of friction (COF) and average wear volume (WV) with their standard deviations (σ) for the tested IPP–based nanolubricants at 393.15 K

Lubricant	COF	σ	WV/10^6 μm^3	σ /10^6 μm^3
10 N				
IPP	0.178	0.014	13.5	1.4
0.25 wt% CNC	0.127	0.003	7.1	1.2
0.5 wt% CNC	0.146	0.013	7.8	1.1
0.75 wt% CNC	0.121	0.013	14.4	1.5
1.0 wt% CNC	0.123	0.014	7.2	1.4
20 N				
IPP	0.067	0.017	16.4	1.9
0.25 wt% CNC	0.056	0.012	13.9	1.2
0.5 wt% CNC	0.063	0.012	11.2	0.8
0.75 wt% CNC	0.049	0.018	16.2	1.5
1.0 wt% CNC	0.055	0.010	13.2	1.6
30 N				
IPP	0.058	0.004	16.4	1.2
0.25 wt% CNC	0.042	0.014	13.6	1.2
0.5 wt% CNC	0.043	0.010	15.2	0.8
0.75 wt% CNC	0.039	0.015	12.7	1.2
1.0 wt% CNC	0.032	0.009	15.7	1.2

Sliding friction

The coefficient of friction was measured during sliding tests for IPP oil and four different mass concentrations of nanolubricants at different loads and at 393.15 K. As shown in Table 3, a decrease in the coefficient of friction (COF) with the increase of the applied load is obtained for both, the neat base oil (IPP) and nanolubricants (IPP + CNCs). The decrease in COF with the load may be attributed to a stronger chemical interaction between the lubricant and the surface, resulting in thinner film lubrication (Muñiz 2022). The percentage reduction in COF was calculated with respect to the average value of the neat base oil (IPP). Figure 5 shows these reductions for each CNC/IPP nanolubricant. All nanolubricants exhibit superior anti-friction behavior compared to the neat IPP base oil. No discernible trend was observed in the mass concentration of the CNCs, consistent with previous reports (Awang et al. 2019a, b; Jason et al. 2020; Yongshun Zhang et al. 2022). However, there is an optimal concentration that results in the maximum reduction in friction. Thus, the highest reductions for each applied load (10 N, 20 N, and 30 N) were

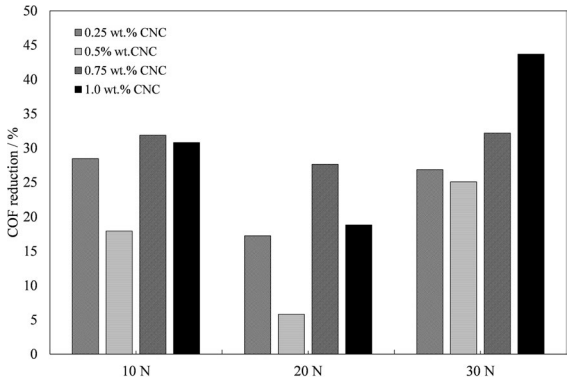

Fig. 5 Reduction of coefficient of friction at 393.15 K obtained in the sliding tests for CNC/IPP nanolubricant at different CNC concentrations

observed for mass concentrations of 0.75 wt%, 0.75 wt%, and 1.0 wt% CNCs, respectively. The 1.0 wt% CNC nanolubricant achieved a maximum COF reduction of 44% under 30 N loading. It should be noted that the observed coefficient of friction reduction is more pronounced at the highest loading (30 N) for all the CNC concentrations. This is because higher loads reduce the thickness of the oil film, which intensifies the lubrication mechanism of the CNC nanoadditives. As a result, cellulose nanocrystals enhance the tribological properties of the neat IPP base oil in these lubrication regimes. In this regard, Awang et al. (2019a, b) have obtained the highest COF reduction (~ 1%) when modifying an SAE 40 engine oil with 0.1 wt% CNCs at 348.15 K, at a constant sliding speed of 500 rpm and a normal load of 39.24 N, while Li et al (2019) obtained the maximum COF reduction (30%) for a PAO additivated with 2 wt% mCNCs at 298.15 K, 20 rpm and 60 N.

The wear volume was quantified using 3D optical profilometry to calculate the wear rate on the worn surface of the disks. Figure 6 displays the grooves obtained for the optimum CNC concentrations under each applied load. The addition of CNCs to the IPP base oil resulted in a clear reduction in wear. The specific wear rate of the disks was calculated using the following equation:

$$WR = \frac{\Delta V}{FS} \tag{1}$$

where WR is the specific wear volume (mm^3 N^{-1} m^{-1}), V is the wear volume (mm^3), and S is the sliding distance (m). The specific wear rate is calculated for all experiments, as depicted in Fig. 7.

It is worth noting in Fig. 7 that, contrary to the expected anti-friction behavior, the wear rate increases with the applied load which is a common phenomenon in tribology (Zhang et al. 2020). Higher loads intensify contact stresses between surfaces, causing slower film formation and leading to greater wear. This effect can be attributed to increased deformation, adhesion, and abrasion between the interacting surfaces. The presence of CNCs at different concentrations appears to have been a key factor influencing wear rates. All concentrations of CNCs reduce the wear rate compared to the neat IPP base oil. Specifically, improvements in wear rate of 47% under 10 N–load (0.25 wt%), 32% under 20 N–load (0.5 wt%), and 25% under 30 N–load (0.75 wt%) are achieved

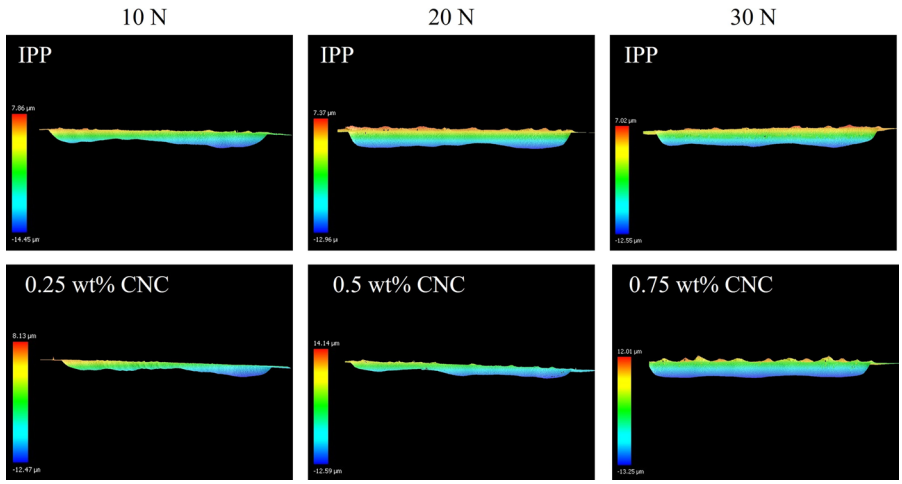

Fig. 6 Optical images of the wear track profile on steel disks under 10, 20, and 30 N loads at 393.15 K

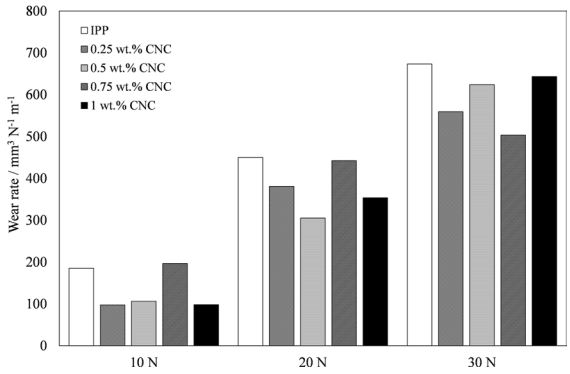

Fig. 7 Wear rate (WR) during sliding tests at 393.15 K for CNC/IPP nanolubricants at different CNC concentrations

for CNCs/IPP nanolubricants. The nanolubricant with 0.25 wt% CNCs under 10 N load achieved the maximum reduction of 47% for antiwear performance. The decline in the coefficient of friction and wear rate may be attributed to the formation of a stable CNC tribofilm (Li et al. 2022b; Lin et al. 2018) on worn surfaces. This tribofilm acts as an ultra-thin surface coating that reduces the shear effect.

Anti-friction/wear mechanisms

Table 4 shows the surface roughness results obtained by 3D optical profilometry for wear tests. As can be seen, for the tests conducted at 10 N, the surface roughness only decreases for the CNC concentration at 0.25 wt% compared with the scar lubricated with neat IPP (from 1.39 to 1.26 µm). This decrease in roughness may explain the outstanding antiwear performance of this concentration (47% WR reduction). For tests conducted at 20 N, all concentrations of CNCs reduced surface roughness. However, the largest decrease (28%) was observed for the 0.5 wt% CNCs, which also exhibited the best antiwear performance. During the friction tests conducted at 30 N, the concentration with the lowest wear rate concentration (0.75 wt%) also resulted in the highest reduction in surface roughness, decreasing it from 1.67 to 1.37 µm. Thus, these results confirm that CNCs are capable of polishing effect, reducing the roughness of the worn surfaces, and minimizing wear. Furthermore, the fibrillar morphology of the CNCs (Fig. 1) implies a high contact surface, reducing the deformation of the rubbing surfaces (Ali et al. 2019) and allows filling the valleys between the asperities (self-repairing mechanisms) to further reduce friction and wear. However, a higher concentration of nanoadditives may be detrimental to the tribological performance of the system, as it can lead to agglomeration of the CNCs in the contact, developing macroparticles that act as inclusions producing an adverse effect (Ettefaghi et al. 2013). No correlation was found between COF and the decrease in surface roughness. This fact is due to that the COF in boundary lubrication is influenced by factors such as the shear strength of the lubricant film and the degree of asperity contact. Thus, when third-body particles are in the contact region, the surface roughness has a negligible influence on the COF (Li et al. 2022).

To detect the function of CNCs in reducing wear, Raman mappings of worn surfaces were recorded with a confocal Raman microscope (532 nm) after friction tests. Prior to the mapping, Raman spectra were obtained for all the components of the nanolubricants, including CNC nanoparticles and neat IPP base oil (Fig. 2), to identify the components in the mapping. Mappings were conducted for worn tracks lubricated with the neat IPP base oil and with the nanolubricant with the best antiwear behavior under a 10 N load, IPP + 0.25 wt% CNCs. Figure 8a shows the relevant areas in red and green, where the spectra correspond to the IPP base oil and iron oxides (Guimarey et al. 2022), respectively.

Table 4 Mean surface roughness (R_a) on the cross-section area of the wear scar on the steel disk and its standard deviation for the neat base oil (IPP) and the nanolubricants

Lubricant	10 N		20 N		30 N	
	Ra / µm	σ / µm	Ra / µm	σ / µm	Ra / µm	σ / µm
IPP	1.39	0.14	1.71	0.40	1.67	0.60
0.25 wt% CNC	1.26	0.06	1.59	0.32	1.45	0.21
0.5 wt% CNC	1.83	0.22	1.24	0.23	2.03	0.51
0.75 wt% CNC	1.48	0.45	1.32	0.11	1.37	0.31
1.0 wt% CNC	1.59	0.36	1.43	0.15	1.66	0.52

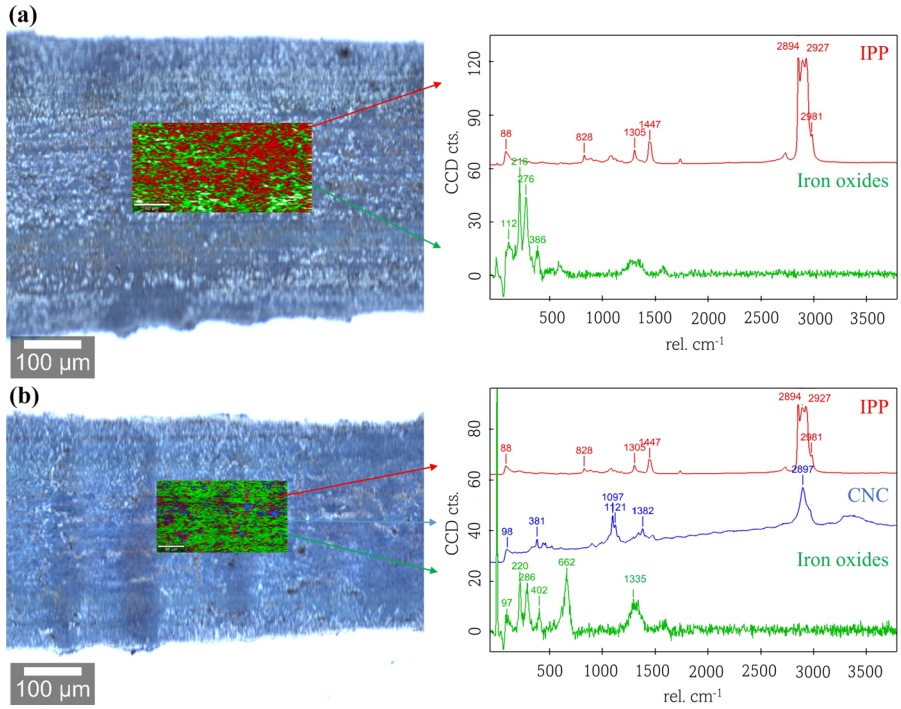

Fig. 8 Mapping Raman of worn surface tested with a) neat IPP base oil, and b) IPP + 0.25 wt% CNC nanolubricant under 10 N-load

The Raman mapping of the track lubricated with the CNC/IPP nanolubricant (Fig. 8b) shows that the spectra obtained in the red and blue areas correspond to that of the neat IPP and CNCs, respectively. This suggests that the self-repairing effect may be attributed to the CNC nanoparticles, which can embed into defects or deformations on the metal surface, thereby performing a surface repair function. Due to the repairing mechanism, nanoparticles can fill the grooves and scars of the rubbing surface, resulting in an improved surface finish (Ali et al. 2016; Çelik et al. 2013; Gulzar et al 2017).

The worn surface of the steel disks lubricated by neat IPP base oil and by IPP + 0.25 wt% CNC nanolubricant was also characterized by high-resolution XPS spectroscopy to analyze the tribomechanism of CNC nanoparticles in the IPP base oil. As shows Fig. 9 the C1s and Fe2p peaks, can be easily identified, appearing in the range 285–287 eV and 706–733 eV, respectively, In Fig. 9a, the Fe A peaks at 706.59 eV (Fe2p3) and 720.39 eV (Fe2p1) are assigned to zero-valent Fe coming from the steel ball (Xu et al. 2024), the Fe B peaks at 708.08 eV (Fe2p3) and 721.44 eV (Fe2p1) are attributed to FeO (Gong et al. 2021), and those Fe C peaks at 709.79 eV (Fe2p3) and 723.09 eV (Fe2p1) are assigned to Fe_2O_3 (Gong et al. 2021). In spite of the low atomic proportion of the metallic iron Fe(0), it can be observed that this signal in the area lubricated with CNC/IPP is practically undetectable (Fig. 9c). This may be an indication that the oxide layer developed in the contact area is thicker in the specimen tested with lubricant incorporating CNCs than in the specimen tested only with neat IPP oil. Thus, CNCs may interact with the steel surface and promote the formation of a passive oxide layer.

Figure 9b, d show the C1s scan spectra on the wear scar lubricated with neat IPP oil and with IPP + 0.25 wt% CNCs, respectively. The carbon atoms give rise to tree photoemission signals (C1s A, C1s B and C1s C) from their different chemical environments. C1s A signal corresponds to C–C and C–H bonds. C1s A signal has 84% relative composition for the wear surface lubricated with neat IPP and 86% for the wear surface lubricated with CNC/IPP nanolubricant. This fact means that the presence of C–C or C–H bonds increases on the wear surface tested with the nanolubricant because the presence of CNCs could form a tribofilm on the surface.

Figure 10 shows the schematic diagram of the friction and wear mechanisms of the CNCs under sliding conditions. The surface investigation revealed the CNC surface enhanced impact through

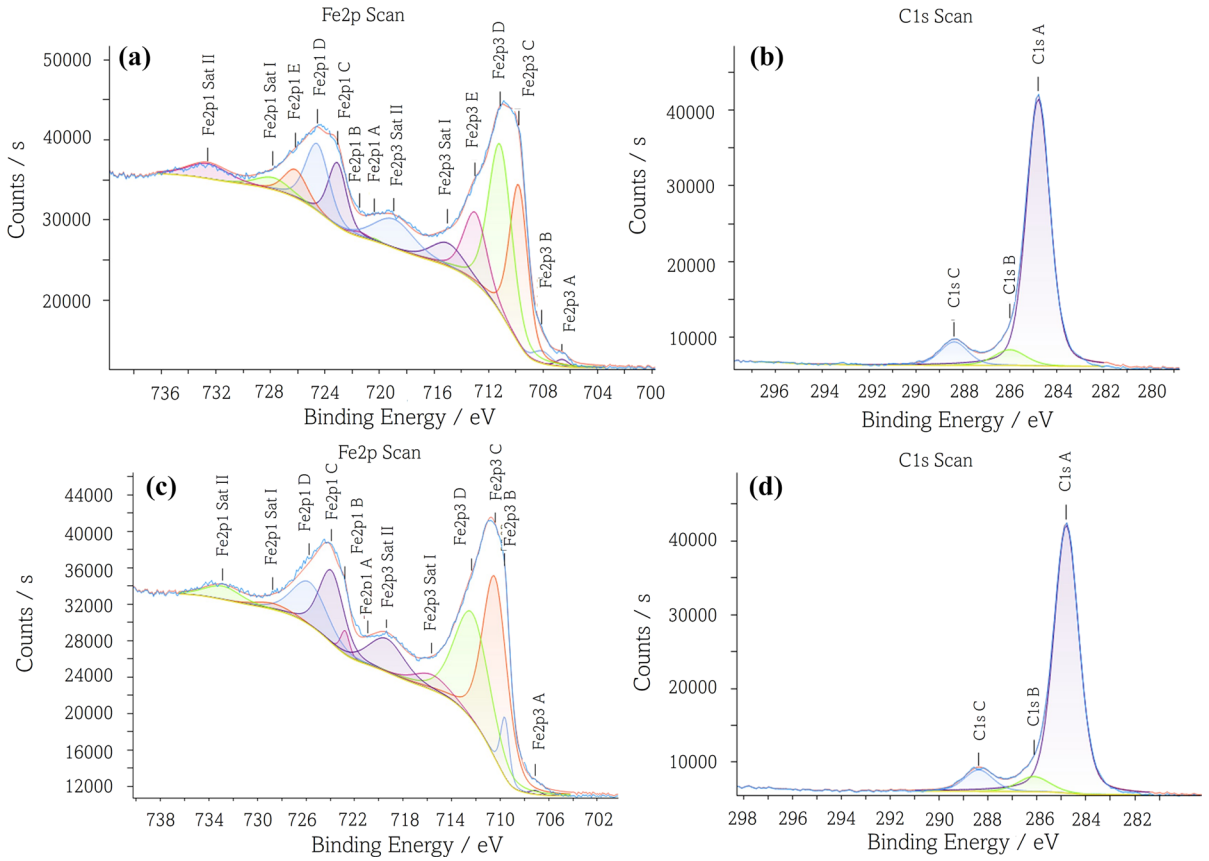

Fig. 9 XPS spectra of Fe2p and C1s elements on worn surface of lower steel disk lubricated with: (**a**, **b**) neat IPP base oil and (**c**, **d**). IPP + 0.25 wt% CNC nanoparticles

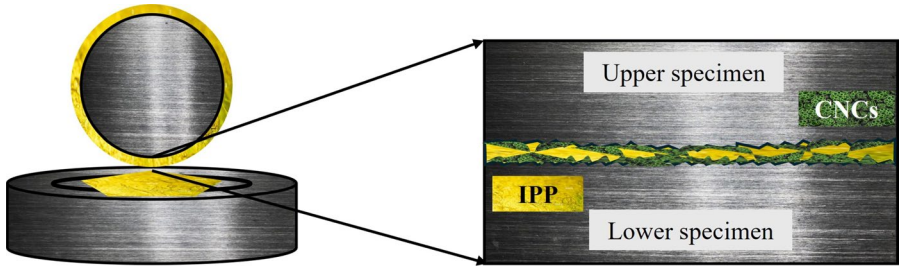

Fig. 10 Schematic diagram of the polishing and self-repairing mechanisms of CNCs under sliding conditions

polishing and mending actions. The fibrillar structure of the CNCs, allows the easy entry of nanoparticles into the contact area and sliding between contact surfaces, increasing the polishing and self-repairing effect on the worn surfaces. Awang et al. (2019a, b) and Li et al. (2019) have also reported good anti-wear ability by the addition of CNCs in engine oil and PAO base oil, respectively, due to mending effect performed by CNCs that allow minimizing surface roughness and asperity contact as well as cover stretches in the worn region.

Rolling-sliding

Figure 11 shows the Stribeck curves for tests conducted with the neat IPP base oil and the nanolubricants at five different temperatures (313.15, 333.15, 353.15, 373.15, and 393.15 K), under 50 N

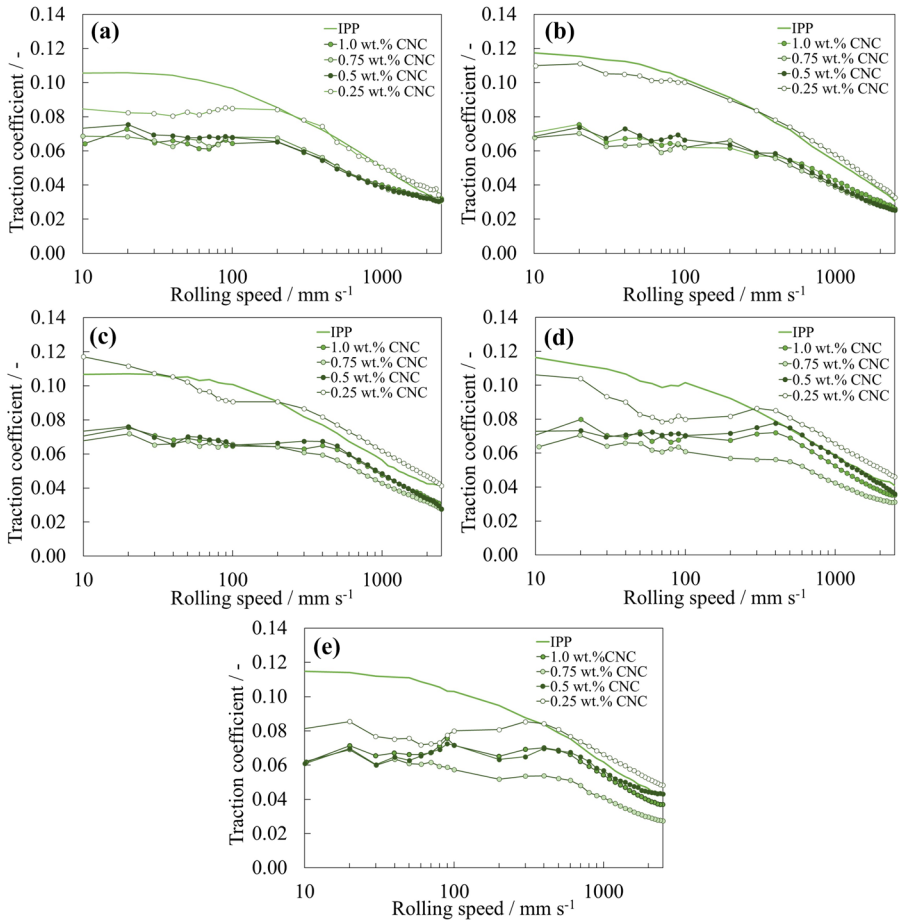

Fig. 11 Stribeck curves from the rolling-sliding friction tests conducted with the neat IPP base oil and the nanolubricants at different CNC concentrations: (**a**) 313.15 K, (**b**) 333.15 K, (**c**) 353.15 K, (**d**) 373.15 K, and (**e**) 393.15 K

and a slide–to–roll ratio (SRR) of 50%. The coefficient of friction (COF) ranges between 0.06 and 0.12 for the lowest speed (10 mm s^{-1}), and between 0.02 and 0.05 for the highest speed (2500 mm s^{-1}) for all samples and temperatures. Thus, it can be observed that the coefficient of friction decreases as the speed increases. In terms of the effect of CNC concentration on COF, the highest and lowest COF reductions were obtained with 0.75 wt% and 0.25 wt% CNCs, respectively, for all test conditions. At a speed of 10 mm s^{-1} and a temperature of 313.15 K, the nanolubricants reduced the COF by 35% (0.75 wt%) and 20% (0.25 wt%) compared to the neat IPP base oil. At a speed of 2500 mm s^{-1} and a temperature of 393.15 K, the 0.75 wt% CNC nanolubricant reduced the COF by 36%, while the 0.25 wt% CNC concentration increased the COF by 13%. Nanoadditives typically improve anti-friction capabilities at low speeds. This is because the boundary regime is more prevalent at lower speeds, resulting in closer contact between the surfaces. As a result, the rod-like nanocrystals of cellulose become trapped in the wear tracks, preventing metal–to–metal contact. Additionally, their high mechanical strength (Mariano et al. 2014; Yu and Yan 2017) promotes friction. Furthermore, the nanoparticles in the lubricant, due to their nanoscale size, assist in filling the gaps between surface irregularities, resulting in a mending or self-repairing effect (Gulzar et al. 2016; Liu et al. 2004). This process facilitates the smoothing of tribopair surfaces, thereby enhancing the anti-friction properties. It is important to note that only the 0.25 wt% CNC loading does not improve the traction behavior to plant–based oil under mixed lubrication (ML). The lower influence of shear and pressure in ML can explain this phenomenon. Additionally, the exfoliation process, which is typical for this type of nanoadditives, may not occur in ML

due to a larger surface separation and lower contact pressure (Rabaso et al. 2014).

Thermal conductivity

Thermal conductivity decreases as temperature increases for both the base fluid (IPP) and all designed nanolubricants, as shown in Fig. 12. IPP thermal conductivity decreases of approximately 5% when the temperature increases from 293 to 333 K. These decreases for nanofluids ranging from 4% for the 0.25 wt% nanolubricant to 7% for the 1 wt% nanolubricant. The increase in CNC content appears to amplify the decrease in thermal conductivity caused by the temperature increase.

The study observed that the thermal conductivity increases as the amount of CNC nanoadditive increases. Specifically, the average increases of 1.6%, 2.5%, 3.5%, and 4.5% were observed for the 0.25, 0.50, 0.75, and 1.0 wt% nanolubricants, respectively. Therefore, it can be concluded that the dispersion of CNCs enhances the thermal conductivity of the neat IPP base oil. This statement is in line with the findings of Farhana et al (2021), who reported a 5.8% enhancement for the 0.5 vol.% dispersion of CNCs in an ethylene glycol:water 40:60 mixture. The concentration with the highest thermal conductivity (1 wt% CNCs) would be expected to exhibit the best anti-friction performance, as observed at 30 N. However, the optimum anti-friction concentration of CNCs achieved at 10 N and 20 N is 0.75 wt%. This fact may be attributed to the experimental conditions, particularly the friction test temperature of 393.15 K. As depicted in Fig. 12, the increase in thermal conductivity becomes less pronounced as the temperature rises, leading to a comparable improvement of thermal conductivity at the different concentrations, approximately converging within the experimental uncertainty between 0.75 and 1 wt% at 393.15 K. Therefore, the thermal conductivity behavior allows to explain the better performance of designed CNC/IPP nanolubricants in terms of preventing excessive heating of the lubricant and the lubricated surfaces. This can reduce friction and wear, leading to improved performance and longevity of the machinery or equipment being lubricated.

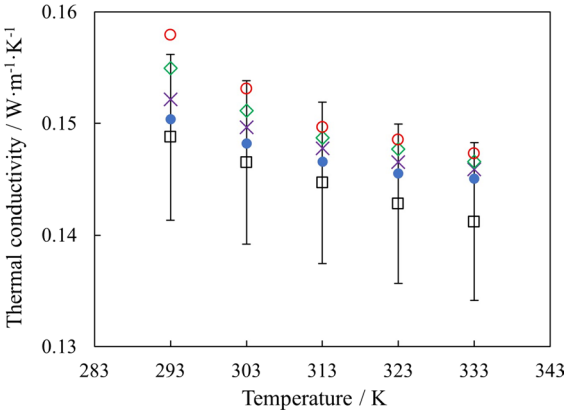

Fig. 12 Thermal conductivity dependence on temperature for: base fluid IPP (square shaped), 0.25 wt% CNC/IPP (blue filled circle), 0.50 wt% CNC/IPP (violet coloured X), 0.75 wt% CNC/IPP (green diamond) and 1.0 wt% CNC/IPP (red ring) nanolubricants. Error bars correspond to 5% uncertainty

Conclusions

This experimental study determined the tribological and thermal properties of dispersed cellulose nanocrystal particles in IPP base oil at CNC concentrations ranging from 0.25 to 1.0 wt%. The main findings of the study are as follows:

(1) Nanolubricants formulated with IPP and CNCs exhibited stability and easily recovered the initial conditions of dispersibility with simple agitation.
(2) The viscous behavior of CNC/IPP nanolubricants demonstrates that lower CNC concentrations enhance the lubricant's thermal stability and performance across a range of temperatures. However, higher concentrations may have a detrimental effect due to potential transitory agglomeration and increased sensitivity to temperature changes.
(3) All CNC/IPP nanolubricants exhibited reduced sliding friction, with the highest reduction observed at 1.0 wt% CNCs under 30 N-load, achieving a friction reduction of up to 44%.
(4) The antiwear capabilities at all CNC concentrations and loading conditions were confirmed. The nanolubricant with 0.25 wt% CNCs under 10 N load showed the best wear rate reduction (47%). This outstanding antiwear performance of CNC-additivated nanolubricants are attributed to the polishing and self-repairing effects of the CNC nanoparticles, particularly noticeable in the

boundary lubrication regime (COF > 0.1) where nanoadditives exhibit enhanced repairing properties.

(5) Increasing the CNC concentration leads to an improvement in the thermal conductivity of the neat IPP base oil, which mitigates excessive heat generation within the lubricant and on the lubricating surfaces, promoting better anti-friction performance under most conditions.

Acknowledgements The authors acknowledge the following institutions and grants for funding this research: Xunta de Galicia (ED431C 2020/10) and MCIN/AEI/https://doi.org/10.13039/501100011033 through the PID2020-112846RB-C21/22 projects. Additionally, Dr M.J.G.G. acknowledges the Xunta de Galicia (Spain) for the postdoctoral fellowship (reference ED481D 2023/016). Dr. M.A.M. acknowledges the financial support by the Ministerio de Universidades (Spain) under budgetary implementation 33.50.460A.752 and by the European Union NextGenerationEU/PRTR through a Margarita Salas postdoctoral contract of the Universidade de Vigo (Spain). Dr J.P.V. thanks the Defense University Center at the Spanish Naval Academy (CUD-ENM) for all the support provided for this research.

Author contributions All authors contributed to the study conception and design. Material preparation, data collection, and analysis were performed by M.J.G.G., M.A.M., and J.P.V. The first draft of the manuscript was written by M.J.G.G., and all authors reviewed the manuscript. All authors read and approved the final manuscript.

Funding Open Access funding provided thanks to the CRUE-CSIC agreement with Springer Nature. This research was supported by the Xunta de Galicia (grants number ED431C 2020/10 and ED481D 2023/016) and MCIN/AEI/https://doi.org/10.13039/501100011033through the PID2020-112846RB-C21/22 projects.

Data availability The data that support the findings of this study are available from the corresponding authors upon reasonable request.

Declarations

Conflict of interest The authors declare no competing interests.

Consent for publication The authors hereby consent to publication of the present research work in this journal.

References

Ali MKA, Xianjun H, Elagouz A, Essa FA, Abdelkareem MAA (2016) Minimizing of the boundary friction coefficient in automotive engines using $Al2O_3$ and TiO_2 nanoparticles. J Nanoparticle Res 18:377. https://doi.org/10.1007/s11051-016-3679-4

Ali I, Basheer AA, Kucherova A et al (2019) Advances in carbon nanomaterials as lubricants modifiers. J Mol Liq 279:251–266. https://doi.org/10.1016/j.molliq.2019.01.113

Aryasena R, Kusmono U, N, (2022) Production of cellulose nanocrystals extracted from Pennisetum purpureum fibers and its application as a lubricating additive in engine oil. Heliyon 8:e11315. https://doi.org/10.1016/j.heliyon.2022.e11315

ASTM International. ASTM D7896–14 Standard test method for thermal conductivity, thermal diffusivity and volumetric heat capacity of engine coolants and related fluids by transient hot wire liquid thermal conductivity method. (2014). In: West Conshohocken, PA, USA: ASTM International.

Awang NW, Ramasamy D, Kadirgama K, Najafi G, Sidik NAC (2019a) Study on friction and wear of Cellulose Nanocrystal (CNC) nanoparticle as lubricating additive in engine oil. Int J Heat Mass Transf 131:1196–1204. https://doi.org/10.1016/j.ijheatmasstransfer.2018.11.128

Awang NW, Ramasamy D, Kadirgama K, Samykano M, Najafi G, Sidik NAC (2019b) An experimental study on characterization and properties of nano lubricant containing Cellulose Nanocrystal (CNC). Int J Heat Mass Transf 130:1163–1169. https://doi.org/10.1016/j.ijheatmasstransfer.2018.11.041

Cabaleiro D, Hamze S, Fal J, Marcos MA, Estellé P, Żyła G (2020) Thermal and physical characterization of peg phase change materials enhanced by carbon-based nanoparticles. Nanomaterials 10:1168. https://doi.org/10.3390/nano10061168

Çelik ON, Ay N, Göncü Y (2013) Effect of nano hexagonal boron nitride lubricant additives on the friction and wear properties of AISI 4140 steel. Part Sci Technol 31:501–506. https://doi.org/10.1080/02726351.2013.779336

Da Rocha PGL, De Oliveira MGL, Lemos PVF, De Sousa Costa LA, Da Rocha LPG, De Almeida Júnior AR, Da Silva JBA (2022) Tribological performances of cellulose nanocrystals in water-based lubricating fluid. J Appl Polym Sci 139:52167. https://doi.org/10.1002/app.52167

Ettefaghi E, Ahmadi H, Rashidi A, Nouralishahi A, Mohtasebi SS (2013) Preparation and thermal properties of oil-based nanofluid from multi-walled carbon nanotubes and engine oil as nano-lubricant. Int Commun Heat Mass Transf 46:142–147. https://doi.org/10.1016/j.icheatmasstransfer.2013.05.003

Farhana K, Kadirgama K, Mohammed HA, Ramasamy D, Samykano M, Saidur R (2021) Analysis of efficiency enhancement of flat plate solar collector using crystal nano-cellulose (CNC) nanofluids. Sustain Energy Technol Assess 45:101049. https://doi.org/10.1016/j.seta.2021.101049

Fernández-Silva SD, Delgado MA, Roman C, García-Morales M (2021) Rheological and Tribological Properties of Nanocellulose-Based Ecolubricants. Nanomaterials 11:2987. https://doi.org/10.3390/nano11112987

Fox NJ, Stachowiak GW (2007) Vegetable oil-based lubricants—a review of oxidation. Tribol Int 40:1035–1046. https://doi.org/10.1016/j.triboint.2006.10.001

Gong K, Lou W, Zhao G, Wu X, Wang X (2021) MoS_2 nanoparticles grown on carbon nanomaterials for lubricating oil additives. Friction 9:747–757. https://doi.org/10.1007/s40544-020-0369-0

Guimarey MJG, Liñeira del Río JM, Fernández J (2022) Improvement of the lubrication performance of an ester base oil with coated ferrite nanoadditives for different material pairs. J Mol Liq 350:118550. https://doi.org/10.1016/j.molliq.2022.118550

Gulzar M, Masjuki HH, Kalam MA, Varman M, Zulkifli NWM, Mufti RA, Zahid R (2016) Tribological performance of nanoparticles as lubricating oil additives. J Nanopart Res 18:223. https://doi.org/10.1007/s11051-016-3537-4

Gulzar M, Masjuki HH, Kalam MA et al (2017) Dispersion stability and tribological characteristics of TiO_2/SiO_2 nanocomposite-enriched biobased lubricant. Tribol Trans 60:670–680. https://doi.org/10.1080/10402004.2016.1202366

Jason YJJ, How HG, Teoh YH, Chuah HG (2020) A Study on the tribological performance of nanolubricants. Processes 8:1372. https://doi.org/10.3390/pr8111372

Kodali DR (2002) High performance ester lubricants from natural oils. Ind Lubr Tribol 54:165–170. https://doi.org/10.1108/00368790210431718

Kumar G, Garg HC (2023a) Evaluation of tribological properties of vegetable oil–based ionanolubricants: An experimental study. Proc Inst Mech Eng Part J 237:1757–1767. https://doi.org/10.1177/13506501231179776

Kumar G, Garg HC (2023b) Tribological evaluation of rice bran oil based ionanolubricants containing ionic liquids and nanoparticles. Tribol Mater Surf Interfaces 17:217–223. https://doi.org/10.1080/17515831.2023.2235234

Kumar G, Garg HC (2024) Dispersion stability analysis of vegetable oil-based ionanolubricants. Proc Inst Mech Eng Part J. https://doi.org/10.1177/13506501241250368

Kumar G, Garg HC (2024) Investigating the Antiwear Characteristics of Castor Oil Based IonanoLubricant Using Four Ball Tester. In: Sinha SK, Kumar D, Gosvami NN, Nalam P (eds) Tribology for energy, environment and society: proceedings of international conference on industrial tribology (ICIT) 2022, (IndiaTrib-2022). Springer, Singapore, pp 91–99. https://doi.org/10.1007/978-981-99-9264-5_8

Li K, Zhang X, Du C et al (2019) Friction reduction and viscosity modification of cellulose nanocrystals as biolubricant additives in polyalphaolefin oil. Carbohydr Polym 220:228–235. https://doi.org/10.1016/j.carbpol.2019.05.072

Li B, Li P, Zhou R, Feng XQ, Zhou K (2022a) Contact mechanics in tribological and contact damage-related problems: A review. Tribol Int 171:107534. https://doi.org/10.1016/j.triboint.2022.107534

Li J, Lin N, Du C et al (2022b) Tribological behavior of cellulose nanocrystal as an eco-friendly additive in lithium-based greases. Carbohydr Polym 290:119478. https://doi.org/10.1016/j.carbpol.2022.119478

Lin L, Ecke N, Kamerling S et al (2018) Study on the impact of graphene and cellulose nanocrystal on the friction and wear properties of SBR/NR composites under dry sliding conditions. Wear 414–415:43–49. https://doi.org/10.1016/j.wear.2018.07.027

Liu G, Li X, Qin B, Xing D, Guo Y, Fan R (2004) Investigation of the mending effect and mechanism of copper nanoparticles on a tribologically stressed surface. Tribol Lett 17:961–966. https://doi.org/10.1007/s11249-004-8109-6

Liu Z, Zhu G, Dai J, Zhu Y, Lin N (2022) Cellulose nanocrystals as sustainable additives in water-based cutting fluids. Carbohydr Polym 298:120139. https://doi.org/10.1016/j.carbpol.2022.120139

Madanhire I, Mbohwa C (2016) Lubricant additive impacts on human health and the environment. mitigating environmental impact of petroleum lubricants. Springer, Cham, pp 17–34

Marcos MA, Cabaleiro D, Guimarey MJG, Comuñas MJP, Fedele L, Fernández J, Lugo L (2018) PEG 400-based phase change materials nano-enhanced with functionalized graphene nanoplatelets. Nanomaterials 8:16. https://doi.org/10.3390/nano8010016

Marcos MA, Cabaleiro D, Hamze S, Fedele L, Bobbo S, Estellé P, Lugo L (2020) NePCM based on silver dispersions in poly(ethylene glycol) as a stable solution for thermal storage. Nanomaterials 10:19. https://doi.org/10.3390/nano10010019

Marcos MA, Fal J, Vallejo JP, Żyła G, Lugo L (2023) Thermophysical, rheological and dielectric behaviour of stable carbon black dispersions in PEG200. J Mol Liq 391:123216. https://doi.org/10.1016/j.molliq.2023.123216

Mariano M, El Kissi N, Dufresne A (2014) Cellulose nanocrystals and related nanocomposites: Review of some properties and challenges. J Polym Sci Part b: Polym Phys 52:791–806. https://doi.org/10.1002/polb.23490

Muñiz, CS (2022) Caracterización tribológica y de corrosión al cobre de fluidos de transmisión con distintas concentraciones de aditivos para vehículos eléctricos. Tecnologías Marinas y Mantenimiento Master Thesis, Universidad de Oviedo

Pownraj C, Valan Arasu A (2021) Effect of dispersing single and hybrid nanoparticles on tribological, thermo-physical, and stability characteristics of lubricants: a review. J Therm Anal Calorim 143:1773–1809. https://doi.org/10.1007/s10973-020-09837-y

Rabaso P, Dassenoy F, Ville F et al (2014) An investigation on the reduced ability of IF-MoS_2 nanoparticles to reduce friction and wear in the presence of dispersants. Tribol Lett 55:503–516. https://doi.org/10.1007/s11249-014-0381-5

Roohpour N, Wasikiewicz JM, Moshaverinia A, Paul D, Rehman IU, Vadgama P (2009) Isopropyl myristate-modified polyether-urethane coatings as protective barriers for implantable medical devices. Materials 2:719–733. https://doi.org/10.3390/ma2030719

Satha H, Kouadri I, Benachour D (2020) Thermal, structural and morphological studies of cellulose and cellulose nanofibers extracted from bitter watermelon of the cucurbitaceae family. J Polym Environ 28:1914–1920. https://doi.org/10.1007/s10924-020-01735-6

Vallejo JP, Mercatelli L, Martina MR, Di Rosa D, Dell'Oro A, Lugo L, Sani E (2019) Comparative study of different functionalized graphene-nanoplatelet aqueous nanofluids for solar energy applications. Renew Energy 141:791–801. https://doi.org/10.1016/j.renene.2019.04.075

Woma TY, Lawal SA, Abdulrahman AS, Olutoye MA, Ojapah MM (2019) Vegetable oil based lubricants: challenges and prospects. Tribol Online 14:60–70. https://doi.org/10.2474/trol.14.60

Xu W, Yang G, Zhang S et al (2024) Tribological properties and tribomechanism of nickel nanoparticles in-situ synthesized in rapeseed oil. Friction 12:474–489. https://doi.org/10.1007/s40544-023-0776-0

Yosief HO, Sarker MI, Bantchev GB, Dunn RO (2023) Isopropyl-branched lard and its potential application as a bio-based lubricant. Lubr Sci 36:104–118. https://doi.org/10.1002/ls.1673

Yu HY, Yan CF (2017) Mechanical properties of cellulose nanofibril (CNF)- and cellulose nanocrystal (CNC)-based nanocomposites. In: Kargarzadeh IAH, Thomas S, Dufresne A (eds) Handbook of nanocellulose and cellulose nanocomposites. Wiley, pp 393–443

Zhang Y, Wei L, Hu H et al (2018) Tribological properties of nano cellulose fatty acid esters as ecofriendly and effective lubricant additives. Cellulose 25:3091–3103. https://doi.org/10.1007/s10570-018-1780-9

Zhang X, Zhu S, Shi T, Ding H, Bai Y, Di P, Luo Y (2020) Preparation, mechanical and tribological properties of WC-Al_2O_3 composite doped with graphene platelets. Ceram Int 46:10457–10468. https://doi.org/10.1016/j.ceramint.2020.01.045

Zhang Y, Xu S, Zhao Z, Shi J, Zhao Y, Zhang G, Wu Z (2022) Mass-produced Cu nanoparticles as lubricant additives for reducing friction and wear. Lubr Sci 34:235–246. https://doi.org/10.1002/ls.1585